University of Kent

Kent Academic Repository

Dolata, Katarzyna M., Montero, Isabel Guerrero, Miller, Wayne, Sievers, Susanne, Sura, Thomas, Wolff, Christian, Schlüter, Rabea, Riedel, Katharina and Robinson, Colin (2019) ***Far-reaching cellular consequences of tat deletion in Escherichia coli revealed by comprehensive proteome analyses.*** **Microbiological Research, 218 . pp. 97-107. ISSN 0944-5013.**

Downloaded from

https://kar.kent.ac.uk/70187/ The University of Kent's Academic Repository KAR

The version of record is available from

https://doi.org/10.1016/j.micres.2018.10.008

This document version

Publisher pdf

DOI for this version

Licence for this version

CC BY (Attribution)

Additional information

Versions of research works

Versions of Record

If this version is the version of record, it is the same as the published version available on the publisher's web site. Cite as the published version.

Author Accepted Manuscripts

If this document is identified as the Author Accepted Manuscript it is the version after peer review but before type setting, copy editing or publisher branding. Cite as Surname, Initial. (Year) 'Title of article'. To be published in *Title of Journal* , Volume and issue numbers [peer-reviewed accepted version]. Available at: DOI or URL (Accessed: date).

Enquiries

If you have questions about this document contact ResearchSupport@kent.ac.uk. Please include the URL of the record in KAR. If you believe that your, or a third party's rights have been compromised through this document please see our Take Down policy (available from https://www.kent.ac.uk/guides/kar-the-kent-academic-repository#policies).

Microbiological Research 218 (2019) 97–107

Contents lists available at ScienceDirect

Microbiological Research

journal homepage: www.elsevier.com/locate/micres

Far-reaching cellular consequences of *tat* deletion in *Escherichia coli* revealed by comprehensive proteome analyses

Katarzyna M. Dolata[a,1], Isabel Guerrero Montero[b,1], Wayne Miller[b], Susanne Sievers[a], Thomas Sura[a], Christian Wolff[a], Rabea Schlüter[c], Katharina Riedel[a,*], Colin Robinson[b]

[a] Institute of Microbiology, University of Greifswald, Felix-Hausdorff-Straße 8, 17487 Greifswald, Germany
[b] School of Biosciences, University of Kent, Canterbury CT2 7NJ, UK
[c] Imaging Center of the Department of Biology, University of Greifswald, Friedrich-Ludwig-Jahn-Str. 15, 17487 Greifswald, Germany

ARTICLE INFO

Keywords:
E. coli
Protein secretion
Twin-arginine translocation
Proteomics
Stress response

ABSTRACT

In *Escherichia coli*, the Twin-arginine translocation (Tat) pathway secretes a set of folded proteins with important physiological functions to the periplasm and outer membrane. The loss of Tat secretion impairs outer membrane integrity and leads to decreased cell growth. Only recently, the Tat pathway has gained more attention due to its essential role in bacterial virulence and applications in the production of fully folded heterologous proteins. In this study, we investigated the influence of the deletion of all active Tat pathway components on the *E. coli* cells. The comprehensive proteomic analysis revealed activation of several stress responses and experimentally confirmed the dependence of certain proteins on the Tat system for export. We observed that a *tat* deletion triggers protein aggregation, membrane vesiculation, synthesis of colanic acid and biofilm formation. Furthermore, the mislocalization of Tat-dependent proteins disturbs iron and molybdenum homeostasis and impairs the cell envelope integrity. The results show that the functional Tat pathway is important for the physiological stability and that its dysfunction leads to a series of severe changes in *E. coli* cells.

1. Introduction

The main systems transporting proteins across plasma membranes in bacteria are highly conserved. Most of the transported proteins are inserted into the membrane or exported to the periplasm via one of the three routes – the Sec machinery, the YidC insertase and the Tat system (Collinson et al., 2015; Lee et al., 2006; Petriman et al., 2018). In *E. coli*, most proteins are transported by the general secretory (Sec) pathway, yet a subset of periplasmic proteins are reported to be exported via the twin-arginine (Tat) pathway (Tullman-Ercek et al., 2007). These two systems use very different mechanisms to transport proteins to the periplasm; the Sec pathway transports proteins in an unfolded state, while the Tat pathway is highly selective for the transport of fully folded proteins (Berks, 2015; Müller and Klösgen, 2005). Remarkably, the Tat system can not only transport folded proteins, but also discriminate against misfolded proteins (Sutherland et al., 2018). This interesting feature implies the existence of a so-called proofreading and quality control mechanism that recognizes correctly folded proteins. However, despite growing research interest, not much is known so far about this mechanism.

Unlike the quality control mechanism, the composition of the Tat translocon is well known. In *E. coli*, the Tat system comprises of four functionally individual membrane proteins - TatA, TatB, TatC and TatE (Bogsch et al., 1998; Patel et al., 2014). TatC is the most conserved of the Tat proteins and contains six transmembrane helices (Behrendt et al., 2004), whereas TatA/B/E are sequence-related and possess a single N-terminal transmembrane α-helix (Baglieri et al., 2018; Koch et al., 2012). Proteins TatC and TatB form a complex, which acts as an initial recognition site for Tat substrates. TatA is a putative pore forming component that may mediate the actual protein translocation event (Fröbel et al., 2012). This complex is recruited to the TatBC complex upon substrate binding (Rose et al., 2013). The amino acid sequences of TatA and TatE are more than 50% identical but these proteins have overlapping functions, with TatB tightly bound to TatC in the substrate-binding complex. It has been shown that the stoichiometry of the TatA/B/C components is crucial for the Tat pathway

Abbreviations: Tat, twin-arginine translocation; Sec pathway, general secretory pathway; cps, capsular polysaccharide; psp, phage shock protein; Fur, ferric uptake regulator

* Corresponding author.
E-mail address: riedela@uni-greifswald.de (K. Riedel).
[1] These authors contributed equally to this work.

https://doi.org/10.1016/j.micres.2018.10.008
Received 5 July 2018; Received in revised form 21 October 2018; Accepted 27 October 2018
Available online 01 November 2018
0944-5013/ © 2018 The Authors. Published by Elsevier GmbH. This is an open access article under the CC BY-NC-ND license (http://creativecommons.org/licenses/BY-NC-ND/4.0/).

functioning (Leake et al., 2008), and an appreciable increase in the Tat-dependent protein flux is possible only when *tatABC* are jointly over-expressed (Alami et al., 2002; Browning et al., 2017). Moreover, a range of *tat* mutants have been constructed to study the roles of Tat pathway components and determine their phenotypes (Lee et al., 2002; Wexler et al., 2000). These studies suggest that both TatB and TatC are essential components of the Tat system and their deletion leads to complete mislocalization of selected Tat substrates. Furthermore, TatB has a function in stabilizing TatC since both proteins are suggested to form a complex. On the contrary, single Δ*tatA* or Δ*tatE* mutations exhibit diverse defects, but no complete dysfunction in Tat-transported protein localization. However, despite the number of studies analyzing *tat* mutants and focusing on the cellular consequences of the Tat secretion impairment in *E. coli*, none of them investigated the cell phenotype under simultaneous deletion of all *tatABCDE* genes.

The Tat pathway operates independently of the Sec and YidC post-translational protein transport systems. Proteins are targeted to the Tat apparatus by an N-terminal signal sequence containing a highly-conserved RR motif that is critical for efficient recognition of Tat substrates (Alami et al., 2003; Stanley et al., 2000). However, it has been shown that signal sequences with a single mutation of an arginine residue are still transported by the Tat system (Ize et al., 2002; Summer et al., 2000). In *E. coli*, at least 29 secreted proteins are predicted to be Tat-dependent. These proteins are involved in important functions e.g. energy metabolism, substrate uptake, cell envelope structure and pathogenicity (Berks et al., 2005; Tullman-Ercek et al., 2007). Interestingly, some of the redox proteins are reported to be transported via the Tat pathway yet they do not have a signal sequence of their own. These proteins use a so-called ''hitchhiker mechanism'' and form a multimeric complex with another protein containing a Tat signal (Rodrigue et al., 1999).

Recently, attention has been attracted by the application of Tat-dependent transport in protein expression and engineering. The Tat pathway is a promising tool for export of complex recombinant proteins and native *E. coli* proteins that fail to be secreted via the Sec pathway (Tinker et al., 2005; Walker et al., 2015). In particular, the proofreading mechanism allows for easier downstream purification as there is less protein heterogeneity in the periplasm sample. Moreover, the role of the Tat pathway in bacterial pathogenesis is under investigation (Ball et al., 2016; Pradel et al., 2003; Ochsner et al., 2002). Although the Tat protein export system is not essential for the growth of *E. coli*, the lack of a functioning pathway causes significant growth defects.

Deletion of the Tat system results in mislocalization of Tat-dependent proteins. Among those, amidases AmiA and AmiC were reported to be important for a functional cell envelope phenotype and cell division process (Bernhardt and de Boer, 2003; Ize et al., 2003). Their mislocalization leads to formation of long chains of cells, which appear to be defective in cell separation (Stanley et al., 2001). Despite the clear importance of Tat-dependent secretion in *E. coli*, our understanding of its biophysical underpinnings remains vague.

In this study, we have sought to ascertain at a comprehensive level how *E. coli* responds to a defect in the Tat protein export pathway. The deletion mutant Δ*tatABCDE* has been used to determine the *E. coli* phenotype and proteome alterations under disruption of the Tat pathway. We describe several stress responses and novel phenotypes emerging from the Tat system's deletion. Moreover, we have experimentally identified a range of known Tat substrates and studied their localization.

2. Materials and methods

2.1. Cell culture and fractionation

E. coli strains utilized for this study were MC4100 and a variant of said strain with a full *tatABCD* deletion and a partial *tatE* deletion (Table 1). Five mL Luria Bertani (LB) medium (10 g/L sodium chloride, 10 g/L tryptone, 5 g/L yeast extract) pre-cultures were inoculated from glycerol stocks and grown aerobically overnight at 30 °C, 200 rpm. The next day cultures were diluted to an OD_{600} of 0.05 in 25 mL fresh LB. Cultures were then grown at 37 °C, 200 rpm in 250 mL Erlenmeyer flasks for 5 h. Cells equivalent to a density of OD_{600} of 10 (~12 mL) were taken and fractioned into cytoplasmic (C), membrane (M) and periplasmic (P) samples. Periplasmic (P) fractions were collected using an EDTA/lysozyme/cold osmotic shock method previously described (Randall and Hardy, 1986), with modifications (Pierce et al., 1997). Spheroplasts were further fractionated into cytoplasmic (C) and insoluble/membrane (M) fractions as described earlier (Pierce et al., 1997). Fractions of three biological replicates from each stain were prepared.

2.2. Inclusion bodies preparation

Inclusion bodies (IBs) were separated from bacterial cultures grown in conditions described in the previous section. Cells were grown for 5 h and harvested by centrifugation at 10.000 × *g*, 4 °C for 10 min. Pellets were resuspended in washing buffer (150 mM NaCl, 50 mM Tris − HCl, pH 8.0) and cells were disrupted by French Press (operated at 16.000–18.000 psi) followed by a high-speed centrifugation at 22.000 × *g*. Unbroken cells, large cellular debris and the inclusion body proteins were washed twice with a washing buffer and IBs were isolated as described previously (Joliff et al., 1986). In short, pellets were resuspended in lysis buffer (5 M urea, 50 mM Tris − HCl, pH 8.0), incubated 15 min at room temperature and centrifuged for 30 min at 22.000 × *g*. The supernatant containing denatured proteins of IBs was separated and concentrated using Amicon® Ultra-0.5 centrifugal filters (Millipore).

2.3. Proteomics sample preparation and LC–MS/MS analysis

Protein concentration was determined by the Bicinchoninic Acid (BCA) Protein Assay (Thermo Fisher Scientific). Cytoplasmic proteins (100 µg) were reduced with TCEP, alkylated with iodoacetamide and digested in-solution using trypsin (Muntel et al., 2012). Desalting of peptides prior to mass spectrometry analysis using Stage tips, C18 material (Thermo Fisher Scientific) was performed according to the protocol described earlier (Rappsilber et al., 2007). For absolute protein quantification, a tryptic digest of yeast alcohol dehydrogenase (ADH1, Waters, USA) was added into the samples to a final concentration of 50 fmol/µL. The nanoACQUITY™ UPLC™ system (Waters) was used to separate and introduce peptides into the Synapt G2 (Waters) mass spectrometer. Parameters for liquid chromatography and IMS^E were used as described previously (Zühlke et al., 2016).

Proteins from periplasmic and membrane fractions (30 µg) were separated via 1D SDS-PAGE, the entire gel lanes cut into ten pieces each. Proteins from isolated inclusion bodies (30 µg) were run via 1D SDS-PAGE 5–6 mm into the resolving gel and the bands containing proteins were cut out of the gel. Proteins were digested with trypsin (Promega, USA) overnight. Peptides were purified using ZipTip C18 tips (Millipore). The eluted peptides were subjected to LC−MS/MS analysis performed on a Proxeon nLC 1200 coupled online to an Orbitrap Elite (Thermo Fisher Scientific) mass spectrometer. Peptides were separated on in-house self-packed columns (id 100 µm, od 360 µm, length 200 mm; packed with 3.6 µm Aeris XB-C18 reversed-phase material (Phenomenex)) in an 80 min nonlinear gradient from 1% acetonitrile and 0.1% acetic acid to 95% acetonitrile, 0.1% acetic acid. To obtain a better separation of peptides of the IBs fraction, peptides were separated on in-house self-packed columns (id 100 µm, od 360 µm, length 200 mm; packed with ReproSil-Pur 120 C18-AQ, 3 µm material (Maisch)) in a 180 min nonlinear gradient. A full MS scan (resolution of 60,000) was acquired using the automatic data-dependent mode of the instrument. After acquisition of the full MS spectra, up to 20 dependent scans (MS/MS) were performed according to precursor intensity by

Table 1
Strains and plasmids used in this work.

Strains	Description	Reference/source
MC4100	AraR, F2 araD139 DlacU169 rpsL150 relA1 flB5301 deoC1 ptsF25 rbsR	Wexler et al. (2000)
Δ*tatABCDE* (Δ*tat*)	MC4100 strain lacking *tatABCDE* genes, AraR	Wexler et al. (2000)

collision-induced dissociation fragmentation (CID) in the linear ion trap. The mass spectrometry proteomics data have been deposited to the ProteomeXchange Consortium (http://proteomecentral.proteomexchange.org) via the PRIDE partner repository with the dataset identifier PXD008803 (username: reviewer18233@ebi.ac.uk, password: FfgJJudJ).

2.4. Protein identification and quantification

MS/MS spectra of cytoplasmic samples were searched against an *E. coli* K12 MC4100 UniProt/Swissprot database (Proteome ID: UP000017782, 3985 protein entries, version January 2017) with added laboratory contaminants and yeast ADH1 sequence (Zühlke et al., 2016). MS/MS spectra of periplasmic and membrane samples were searched against the above-mentioned database using MaxQuant software (version 1.5.8.3) (Cox and Mann, 2006). The search was performed with the Andromeda search algorithms (Cox et al., 2011). Search parameters were set as follows: a minimal peptide length of six amino acids, up to two missed cleavages, carbamidomethylation of cysteine specified as a fixed modification, N-terminal protein acetylation and methionine oxidation were set as variable modifications. The false discovery rate (FDR) was estimated and protein identifications with FDR < 1% were considered acceptable. A minimum of two unique peptides per protein was required for relative quantification using the label free quantification (LFQ) algorithm provided by MaxQuant.

2.5. Protein functional analysis and subcellular localization prediction

The Student's *t*-test requiring a p-value of < 0.05 was subsequently conducted to determine proteins with significant alterations in protein abundance. Changes in protein abundance of Δ*tat* vs. wild type (WT) were presented with a log2 fold change (Supplementary Table 1). If the proteins were identified in only one of the strains in three biological replicates, they were added to the list of ON/OFF proteins. Heat maps were generated with Prism 7 (GraphPad) and the protein biological functions were assigned based on their FIGfam roles according to The SEED (http://pubseed.theseed.org/) (Overbeek et al., 2014) complemented with manual curation. The protein subcellular localization was assigned based on the *E. coli* specific STEP database (STEPdb) (Orfanoudaki and Economou, 2014).

2.6. Transmission electron microscopy (TEM)

Cells were fixed (1% glutaraldehyde, 4% paraformaldehyde, 0.2% picric acid, 50 mM sodium azide in 5 mM HEPES buffer pH 7.4) at 4 °C and stored at the same temperature until further processing. Subsequently to embedding in low gelling agarose, cells were postfixed in 2% osmium tetroxide in washing buffer (50 mM cacodylate buffer pH 7, 10 mM magnesium chloride, 10 mM calcium chloride) for 1 h at 4 °C. After dehydration in a graded series of ethanol (20%, 30%, 50% for 10 min each step; 70% ethanol with 0.5% uranyl acetate for 30 min at 4 °C; 90%, 96%, 100% ethanol) the material was embedded in AGAR 100 resin. Sections were cut on an ultramicrotome (Reichert Ultracut, Leica UK Ltd, Milton Keynes, UK), stained with 4% aqueous uranyl acetate for 3 min followed by lead citrate for 1 min and analyzed with a transmission electron microscope LEO 906 (Zeiss, Oberkochen, Germany). Afterwards, the micrographs were edited by using Adobe Photoshop CS6.

2.7. Crystal violet biofilm assay

A quantitative biofilm assay was performed in 96-well polystyrene plates as described previously (O'Toole, 2011). Briefly, cells were inoculated from overnight cultures grown in LB and Belitsky minimal medium (Stülke et al., 1993), diluted in replicates in both media to an initial turbidity of 0.05 at 600 nm and grown at 37 °C without shaking. Cell density (turbidity at 600 nm) was measured after 24 and 48 h in a microtiter plate reader (BioTek Synergy™ Mx) and analyzed with Gen5™ version 2.0 software. After removing the supernatants, biofilms were stained with crystal violet and absorbance at 550 nm was measured. Total biofilm was normalized by bacterial growth for each strain and represented as biofilm formation index (BFI). Each data point was averaged from at least 20 replicate wells.

2.8. Quantification of colanic acid

Colanic acid was quantified by measuring L-fucose, the sugar component which is exclusively found in this exopolysaccharide (EPS) (Stevenson et al., 1996). Samples of *E. coli* biofilm, growing in the wells of 6-well polystyrene plates for 48 h, were collected and colanic acid concentration was measured based on previously described method (Obadia et al., 2007). Biofilm samples were boiled for 15 min to inactivate EPS-degrading enzymes and release EPS from the cell surface. In the next step, samples were centrifuged at 14.000 x g for 30 min at 4 °C, after cooling down to room temperature. The supernatants were collected, and polysaccharides were precipitated with 70% ethanol overnight. Samples were subjected to centrifugation at 14.000 × *g* for 30 min at 4 °C. The pellet was diluted to 0.2 mL with distilled water and mixed with 0.8 mL of H_2SO_4/H_2O (6:1; v/v). The mixture was heated at 100 °C for 20 min and cooled down to room temperature. For each sample, absorbance at 396 nm and 427 nm, before and after addition of 100 µL of cysteine hydrochloride, was measured. The absorption due to this reaction was subtracted from the total absorption of the sample, as described earlier (Obadia et al., 2007). A L-fucose (Sigma-Aldrich) calibration curve was used (0–100 µg/mL) to determine the fucose concentration. The values for *E. coli* biofilm samples were normalized by cell turbidity at 600 nm.

3. Results and discussion

3.1. Comparative proteomic analysis of E. coli subfractions

In this study, we carried out a comparative proteomic analysis of *E. coli* wild type and Δ*tatABCDE* strains. To efficiently identify and quantify proteomic changes, three different subcellular fractions were investigated, i.e. periplasmic and cytoplasmic protein fractions as well as an insoluble protein fraction containing mainly membrane proteins. The application of subcellular compartment fractionation was previously shown to improve protein identification, especially for membrane and periplasmic proteins (Brown et al., 2010). However, the common limitation of subfractionation methods are the impurities of highly abundant cytoplasmic proteins in periplasmic and membrane fractions (Brown et al., 2010; Wolff et al., 2008). To validate a high resolution and good depth coverage of periplasmic and membrane proteins in the subcellular fractions, we have calculated the abundance of protein impurities in all the fractions based on signal intensities (Table 2). As expected, the analysis of relative protein abundances

Table 2
Distribution of enriched proteins and protein impurities observed in subcellular fractions via LC–MS/MS.

Cell fraction	*E. coli* MC4100		*E. coli* MC4100 Δ*tat*	
	Total recovery [%][a]	Protein impurities [%][b]	Total recovery [%][a]	Protein impurities [%][b]
Cytoplasm	76.58	23.42	73.23	26.77
Periplasm	66.88	33.12	31.75	68.25
Membrane	66.88	33.12	50.27	49.73

[a] Total recovery shows the percentage of the total abundance, calculated from LFQ intensities, of proteins identified in a certain subfraction and assigned to this subfraction by STEPdb.

[b] Protein impurities shows the percentage of the total abundance, calculated from LFQ intensities, of proteins identified in a certain subfraction but assigned to other subfractions by STEPdb.

points to cross-contamination in all the subfractions of *E. coli* MC4100 and to significantly higher levels of cytoplasmic contaminants for membrane and periplasmic fractions of the *E. coli* Δ*tat* mutant. These results are not surprising, given the fact that some *tat* deletion strains have been reported to present cell envelope disruption and cytoplasmic protein leakage (Ize et al., 2003). Based on the high content of cytoplasmic proteins in the periplasmic fraction of the *E. coli* Δ*tatABCDE*, but not the control strain, we conclude that the complete deletion of the Tat system leads to a disruption of the inner membrane and cytoplasmic protein leakage during fractionation. Collectively, our results indicate that the fractionation protocol distinctively enriched subcellular fractions, however, due to the Δ*tat* membrane impairment, it was not possible to obtain a comparable protein enrichment rate for both strains.

3.2. Pleiotropic effects in an E. coli tat mutant

Various reports have demonstrated that Δ*tatAE* and Δ*tatC E. coli* mutants display pleiotropic phenotypes. The most prominent effect of the Tat-system impairment is the formation of filamentous, chain like structures (Fig. 1), comprised of cells which fail to undergo a complete cell division (Stanley et al., 2001). This phenotype is assumed to be the result of mislocalization of amidases AmiA and AmiC. Both proteins are involved in splitting the murein septa and the separation of cells. It has been shown that the chain forming phenotype can be complemented by overexpression of AmiB (Bernhardt and de Boer, 2003). Here, we decided to investigate if the simultaneous deletion of *tatABCDE* will contribute to the discovery of novel phenotypes of the *E. coli tat* mutants.

In addition to previously reported findings, this study revealed an increase in inclusion body formation (Fig. 1B) and membrane vesiculation in the *E. coli tat* mutant (Fig. 1C) compared to the wild type (Fig. 1A). Inclusion body formation occurs naturally in bacteria as a result of the accumulation of unfolded proteins. In our study, the *tat* mutant strain formed inclusion body-like aggregates in moderately higher amounts than the wild type. Thus, we conducted a proteomic analysis to investigate whether there is any difference in the composition of the IB fraction between the wild type and the mutant (Supplementary Table 2). Several cytoplasmic proteins such as GroEL and DnaK, the main drivers of protein folding (in concert with their co-chaperones DnaJ-GrpE and GroES, respectively), IbpA and ClpB have been found to be more abundant in the IB fraction of the mutant strain compared to the WT. Together, these proteins have been already identified as real cytoplasmic components of *E. coli* IBs (Carrio and Villaverde, 2002) and GroEL itself may promote IBs formation via clustering of small aggregates. Interestingly, we could identify the cell division protein ZipA in Δ*tat* IBs. This protein is essential for cell division, as it binds with FtsZ protein and forms the septal ring structure that mediates cell division in *E. coli* (Brown et al., 2010). Together with the mislocalization of AmiA and AmiC, the lack of functioning of ZipA may contribute to the formation of long-chains of cells in the *E. coli* Δ*tat* mutant.

The second novel phenotype we observed in Δ*tat E. coli* cells was the formation of outer membrane vesicles (OMV). Several cells formed OMVs, especially the cells who failed to undergo complete division (Fig. 1C). This phenotype is most likely induced in response to the state of the cell envelope and the accumulation of overexpressed or misfolded proteins. In conclusion, the Δ*tatABCDE* mutation in *E. coli* results not only in the formation of long chains of cells, as previously reported for Δ*tatAE* and Δ*tatC* mutants, but also in the production of OMVs and increased formation of IBs, which may serve as a complementary mechanism for managing stress at the cell envelope.

3.3. The effect of Δtat mutation on the export of Tat-dependent substrates

The genome of *E. coli* is predicted to encode between 22 and 34 proteins with a Tat signal peptide (Bendtsen et al., 2005; Dilks et al., 2003; Robinson and Bolhuis, 2001; Tullman-Ercek et al., 2007). These predictions are primarily based on the properties of the signal peptides; however, confirming their status as Tat dependent substrates is difficult due to the fact that some of the signal peptides are also capable of directing export of heterologous proteins to the periplasm through the Sec pathway (Blaudeck et al., 2001, 2003; Stanley et al., 2002) and this pathway is essential for the viability of the cells (Economou, 2005). Current studies have shown that the Tat system is used to directly export 27 proteins to the periplasm and indirectly export another 8 using the hitchhiker mechanism described before (Berks et al., 2005; Tullman-Ercek et al., 2007). Out of the 27 reported, we only identified 8 Tat substrates and 3 of the hitchhiker proteins (Fig. 2). The presence of so few Tat substrates is most likely due to the low stress conditions in which the cells were grown, as well as the phase in which they were harvested (exponential). Many of Tat-dependent proteins have been found to be expressed only under certain conditions such as anaerobic growth (HyaA, HybO, NrfC, TorA and TorZ) (Hussain et al., 1994; Méjean et al., 1994; Sawers and Boxer, 1986), presence of cinnamaldehyde at a low pH (YagT) (Neumann et al., 2009) or hydroxyurea (FhuD) (Davies et al., 2009). The expression of some of the Tat substrates can be also inhibited by other proteins like NarL (YnfE, YnfF, YnfG and once again TorA) and NarP (FdnH) (Constantinidou et al., 2005). The rest of the Tat substrates have been shown not to be essential for the growth conditions tested (SufI, YahJ, MdoD, YaeI, Ycb and FdoH) (Gerdes et al., 2003). Within these 8 identified Tat substrates and 3 hitchhiker proteins we could discern 3 different localization and expression profiles.

The first four proteins examined were HybA, EfeB, AmiA and AmiC as they were found to be exclusively present in the periplasm of the WT, but not in the Δ*tat* strain, strongly suggesting that they are exported exclusively by Tat. HybA and EfeB (previously YcdB) seem to be lacking entirely in all other fractions of Δ*tat* strain, presumably due to degradation in the absence of export. The up-regulation of *hybA* and *efeB* genes expression in the *E. coli* Δ*tatC* strain has been already shown (Ize et al., 2004), thus we assume that the absence of HybA and EfeB in our Δ*tat* mutant might be due to degradation inside the cell. On the other hand, the levels of AmiA and AmiC accumulated in the membrane fraction of the WT as well as in the Δ*tat* mutant. This suggests that there is an inherent stability in these proteins that allows for an excess of protein to associate with the membrane without sequestration in insoluble bodies. When analyzing the content of IBs formed in the Δ*tat* strain, no traces of these proteins were determined. This suggests that their presence in the membrane fraction is due to the association of these proteins with the inner membrane of the cells, but not in inclusion bodies.

Another two Tat dependent substrates, CueO and NapA, were identified in the periplasm of the Δ*tat* strain. However, they were not as

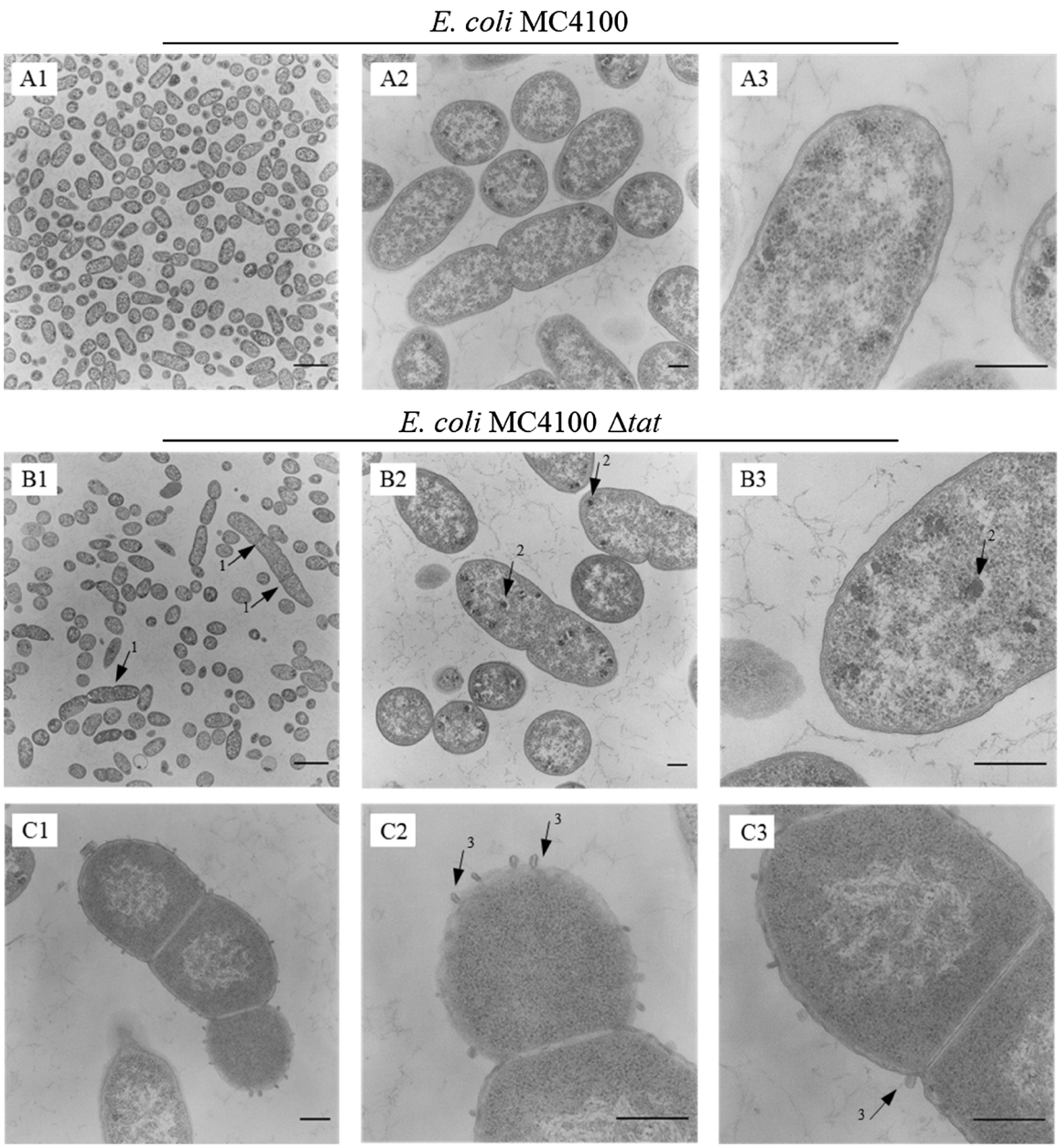

Fig. 1. Transmission electron micrographs of *E. coli* MC4100 (WT) (A1-A3) and Δ*tat* (B1-B3, C1–C3) strains at different magnifications.
The cells were grown aerobically in LB medium for 5 h. The mutant strain shows morphological changes such as formation of 1. Long chains of cells, 2. Inclusion bodies and 3. Outer membrane vesicles. Scale bars A1, B1 = 2 μm; scale bars A2, A3, B2, B3,C1, C2, C3 = 250 nm.

abundant and found in much lower quantity than in the WT, suggesting that instead of using Sec as a secondary translocation mechanism these traces of protein are artifacts of the fractionation process discussed before. When comparing the amount of protein present in WT and mutant, we found that both proteins accumulate in the membrane fraction of the *Δtat* strain. In the case of CueO this accumulation only happens in Δ*tat*, implying that the protein either associates with the membrane or causes aggregation into inclusion bodies.

The next group contains two Tat substrates, FdnG and DmsA. Due to their tight association with inner membrane proteins they are not present in the periplasmic fraction. FdnG is associated with the transmembrane protein FdnI, whereas DmsA form a complex with DmsB and DmsC (Stanley et al., 2002). Both FdnI and DmsC are not present in our samples, probably because of the difficulty to identify transmembrane proteins using the proteomics methods described in this study (Rabilloud, 2012). We observe a dramatic decrease in abundance of FdnG and DmsA in *Δtat* cells. The presence of FdnG and DmsA in the Δ*tat* cells is most likely due to their association to the inner membrane on the cytosolic side. Since we did not identify them in the IB fraction, we assume they do not aggregate.

The final group of Tat substrates are the hitchhiker proteins: DmsB, HyaB and HybC. DmsB is undetected in the *Δtat* cells. Both HyaB and HybC form multimeric complexes with HyaA and HybO, respectively to be correctly co-transported across the membrane with the help of the chaperons HyaE and HybE (Berks et al., 2005; Palmer et al., 2005). Neither HyaA nor HybO were identified, although they are both located upstream in their operons, followed by their hitchhiker counterparts. However, both of these proteins have transmembrane domains (Hatzixanthis et al., 2003) meaning that, as described before, their identification is analytically challenging. HyaB was not present in *Δtat* cells and HybC was downregulated, however the abundance values were not statistically significant. In both cases the amount of protein we

Category	Accession number UniProt	Protein biological function	Protein	Log2 fold change		
				C	M	P
Tat Substrates	P0AAJ8	Hydrogen oxidation	HybA			OFF
	P31545	Iron transport	EfeB			OFF
	P36548	Cell wall amidase	AmiA		1.2 *	OFF
	P63883	Cell wall amidase	AmiC		0.7	OFF
	P36649	Copper homeostasis	CueO		ON	-2.8 ***
	P33937	Nitrate reduction	NapA	0.7	1.2	-12.3 **
Membrane bound Tat substrates	P24183	Formate oxidation	FdnG		-2.7 *	
	P18775	DMSO reduction	DmsA		-7.7 *	
Hitchhiker proteins	P18776	DMSO reduction	DmsB		OFF	
	P0ACD8	Hydrogen oxidation	HyaB	OFF		
	P0ACE0	Hydrogen oxidation	HybC	-1.5		

OFF Identified only in wild type
ON Identified only in Δ*tat*
Increased abundance in Δ*tat*
Decreased abundance in Δ*tat*
Protein not identified

Abbreviation
C- cytoplasmic fraction
M- membrane (insoluble) fraction
P- periplasmic fraction

Data significance (p value)
* P<0.05
** P<0.01
*** P<0.001

Fig. 2. Protein abundance of Tat substrates in *E. coli* Δ*tat vs.* WT.
The table shows Tat substrates their abundance which increased or decreased due to the Tat pathway deletion. Proteins are grouped according to their localization pattern. The functional classification and accession numbers were adopted from UniProt. The average ratios (log2 fold change) of the protein abundance in Δ*tat vs.* WT are shown. The fold change in the abundance is marked with shading; blue – decreased abundance, orange- increased abundance. Significantly different results were marked with asterisks, (*) $P < 0.05$, (**) $P < 0.01$, (***) $P < 0.001$.

expect to find are minimal since both operons are under promotors that are induced under anaerobiosis. It is likely then that both HyaB and HybC are either being produced on their own, or alongside HyaA and HybO, but these last two are degraded before they can be exported since the cells are not under anaerobiosis. Thus, without HyaA and HybO their hitchhikers HyaB and HybC are not able to cross the inner membrane to the periplasm and can accumulate in the cytoplasm in small amounts before being degraded.

3.4. Proteome changes linked to the loss of Tat export

Deactivation of the Tat apparatus causes profound stress in *E. coli* cells. The global analysis of gene regulation has shown the effect of *tatC* deletion on the expression of genes involved in cell envelope associated functions, iron and copper homeostasis and polysaccharide synthesis (Ize et al., 2004). However, to our knowledge, there have been no studies on the effects of *tatABCDE* deletion on the *E. coli* proteome. Thus, in this study we decided to characterize the effect of the loss of all known Tat secretion components on proteins located in the periplasm, membrane, and cytoplasm. A set of 98 proteins related to stress response were identified and represented in the heat map (Fig. 3) (Supplementary Table 3). Changes in protein abundance between the *E. coli tat* mutant and its parental strain were shown as log2 fold changes.

3.4.1. Activation of chaperones and proteases in periplasm

E. coli cells upregulate the expression of chaperones and proteases in response to cellular and environmental stress. We observed that the abundances of several chaperones and proteases were increased in the cytoplasmic and periplasmic fractions of the *tat* mutant cells (Fig. 3A). Among the upregulated chaperones in the cytoplasm, the most prominent increase in the protein abundance was observed for the HscA chaperone which is required for the assembly of iron-sulfur clusters (Takahashi and Nakamura, 1999). Moreover, two of the major chaperone systems DnaK/J/GrpE and GroEL/GroES also become upregulated as a consequence of the *tat* deletion. DnaK is one of the most abundant and essential stress inducible chaperones (Bukau and Walker, 1989), it works together with its co-chaperones DnaJ and GrpE to facilitate de-novo protein folding in stressed *E. coli* cells. GroEL is accompanied by its cofactor GroES, and together they are essential for viability under all growth conditions tested (Fayet et al., 1998). Furthermore, a number of additional proteins, including ClpB, HtpG, IbpA/B and HslO, are induced under stress conditions to prevent and/or repair stress-induced damage in the *E. coli* proteome (Hoffmann et al., 2004; Schröder et al., 1993; Thomas and Baneyx, 2000). Proteases work together with chaperones and form the cell quality control system of *E. coli*. These proteolytic enzymes degrade damaged, misfolded or unassembled polypeptides, which become harmful when accumulated in the cell. The main cytoplasmic proteases such as Lon, ClpP/X and HslV/U are present in the cytoplasmic fraction of *E. coli* Δ*tat* in high amounts. The periplasmic fraction shows activation of DegP/Q proteases. In addition, we observed the increase in the abundance of cytoplasmic proteases and chaperones in the periplasmic fraction of the Δ*tat* (Fig. 3A1). We assume that most of the cytoplasmic proteins observed in the periplasmic fraction are technical impurities of the osmotic shock separation process (Brown et al., 2010; Yaagoubi et al., 1994). However, considering their upregulation in both the cytoplasmic and periplasmic fractions, the induction of chaperones and proteases in the *tat* mutant remains unquestionable. We also hypothesize that the upregulation of some cytoplasmic proteins such as GroEL and DnaK may suggest their actual presence in the periplasm. It has been previously reported that a high load of cytoplasmic aggregates can result in their secretion to the periplasm together with GroEL and DnaK (Mar Carrió and Villaverde, 2005). In conclusion, the observed increase in the abundance of chaperones and proteases is most likely a reaction to the perturbations caused by mislocalization and cytoplasmic accumulation of Tat substrates, and the loss of their function in the cell, which disturbs the whole network of proteins that are directly or indirectly involved in Tat secretion.

3.4.2. Cellular stress responses

Our analysis has also revealed the induction of proteins involved in the stress response to heat, oxidation, changes in osmolarity and cold (Fig. 3B). Interestingly, we observed that PspF, the transcriptional activator of the stress-induced *psp* operon, is present only in the *E. coli tat* mutant. The Psp response is induced by perturbations in the integrity and energization of the inner membrane. PspF initiates the Psp response which has been shown to become active with defects of the Sec secretion system (Jones et al., 2003) and enhances the efficiency of the Tat pathway function (Delisa et al., 2004) when the translocation apparatus becomes saturated. Furthermore, most of the upregulated oxidative stress related proteins were also identified in the periplasmic fraction (Fig. 3B1). For example, thioredoxin TrxC which reduces disulfide

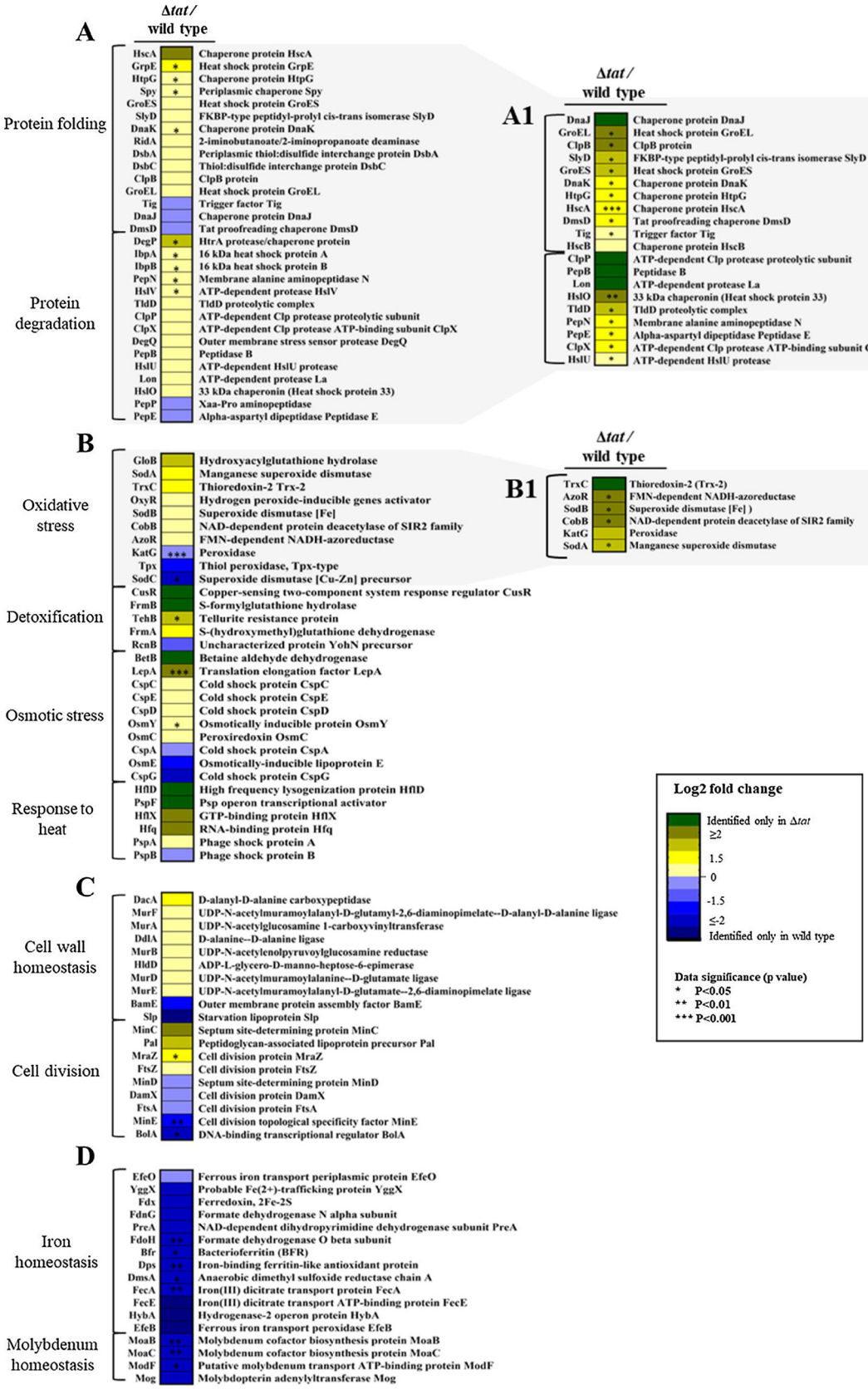

Fig. 3. Heat map of changes in the abundance of stress response proteins between *E. coli* Δ*tat* and the WT.
A set of 98 proteins related to stress responses were categorized into 10 functional groups using Figfam classification. The heat map shows proteins involved in: protein folding and degradation (A, A1), stress responses (B, B1) cell envelope stress and cell division (C) and iron and molybdenum homeostasis (D). Proteins represented in panels A1 and B1 were identified in high abundance in the periplasmic fraction, however according to STEPdb they are cytoplasmic proteins. The changes in protein abundance between *E. coli* Δ*tat* and the parental strain are represented as mean log2 fold change and are depicted in a color gradient from blue (decreased protein abundance in Δ*tat*) to yellow-green (increased protein abundance in Δ*tat*). Significant results were marked with asterisks, (*) $P < 0.05$, (**) $P < 0.01$, (***) $P < 0.001$.

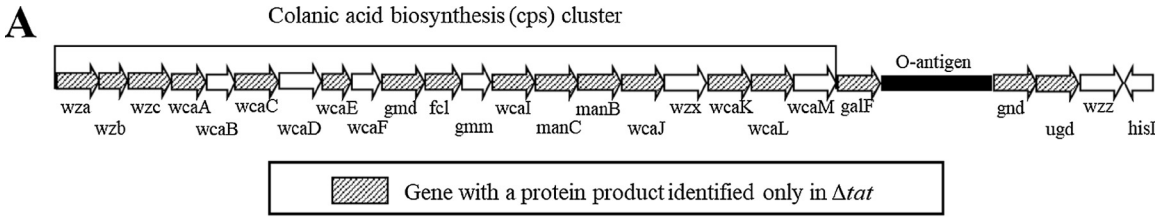

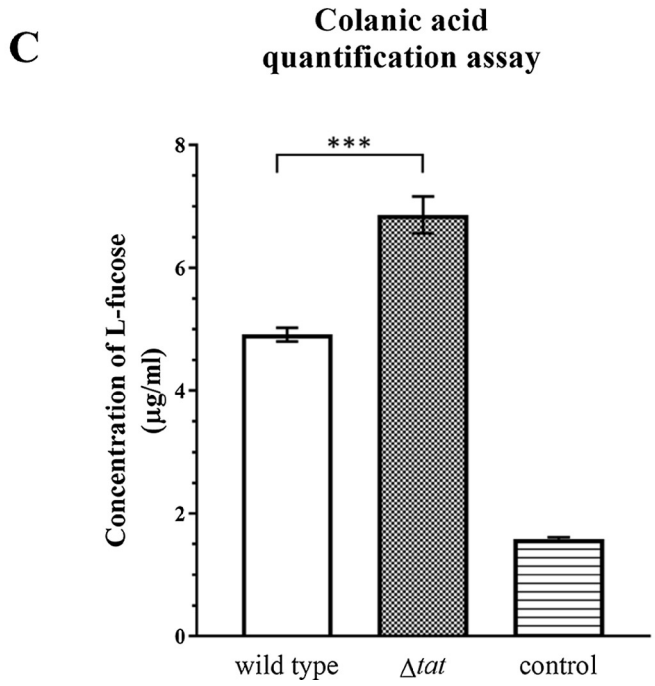

Fig. 4. Induction of colanic acid synthesis in *E. coli* Δ*tat*.
Genetic organization of *E. coli* colanic acid synthesis (*cps*) cluster (A). Genes which protein products were synthesized upon *tat* mutation were marked. Table representing induced proteins of colanic acid synthesis and their cellular localization (B). Concentrations of colanic acid in *E. coli* WT and Δ*tat* grown in LB liquid medium were compared (C). To quantify colanic acid, concentration of its specific component, L-fucose, was measured. LB liquid medium was used as a control. Bars represent geometric means ± standard deviations from three parallel samples. A Student's *t*-test was applied to determine statistical significance, (***) $P < 0.001$.

bridges and methionine sulfoxide formed by reactive oxygen species during the oxidative stress. TrxC is induced by OxyR in the cytoplasm, however it is also present in the periplasm of the *tat* mutant. It has been shown that some small cytoplasmic proteins such as thioredoxin and superoxide dismutase (SodA) can be released from the cytoplasm through the mechanosensitive ion channel of large conductance (MscL) during osmotic shock (Ajouz et al., 1998; Krehenbrink et al., 2011).

3.4.3. Cell envelope stress

It has been previously observed that *E. coli tat* mutants have impaired membrane integrity which results in outer membrane permeability and depletion of peptidoglycans (Ize et al., 2004). One possible explanation for this defect of cell envelope integrity is the mislocalization of amidases AmiA and AmiC, involved in cell wall metabolism. To combat stress resulting from the disruption of the peptidoglycan layer and compensate for its depletion, *E. coli* upregulates proteins involved in the cell wall biogenesis pathway. The proteomic analysis revealed an increased abundance of proteins MurA/B/D/E/F (Fig. 3C), which take part in the synthesis of murein. Most likely, the cell senses the depletion of peptidoglycans in the membrane and escalates their synthesis. In addition, we observed an increase of proteins involved in colanic acid synthesis. This polysaccharide is produced

in response to changes in the environment, that may damage the outer membrane, and it protects the cell capsule of *E. coli* (Gottesman and Stout, 1991). The upregulation of proteins involved in colanic acid synthesis is described in the next Section (3.5). The phenotypic analysis has shown that Δ*tatABCDE*, similar to Δ*tatC* (Ize et al., 2004), is impaired in the cell separation stage of cell division. Here, we identified some important proteins for the cell division process which may be co-responsible for the formation of long chains of cells in the *E. coli tat* mutant. We determined the upregulation of MinC, cell division inhibitor protein (Conti et al., 2015), and MraZ whose overproduction was reported to be lethal and perturb cell division (Eraso et al., 2014). Together with these findings we observed a dramatic downregulation of transcriptional regulator protein BolA which is involved in the coordination of genes that control cell physiology and cell division (Aldea et al., 1988).

3.4.4. Iron and molybdenum homeostasis

The Tat secretion pathway is involved in the transport of iron. Many of the known Tat substrates bind Fe-S cofactors, and EfeB is directly involved in the iron uptake by extracting iron from heme in *E. coli* cells. We believethat *tat* deletion regulatory influences the expression of the ferric citrate transport (*fec*) operon. We observed that FecA is not present in the periplasmic fraction of Δ*tat* and it is significantly downregulated (−10 log2 fold change) in the insoluble fraction. Since FecA binds $(Fe^{3+}$ citrate$)_2$ to the outer membrane and initiates transcription of the *fec* transport genes, its absence in the cell most likely results in cessation of the Fec-dependent transport, which explains the absence of FecE transporter in the *E. coli tat* mutant. In addition, we found several other proteins e.g. YggX, Dps, Bfr, Fdx, PreA and FdoH, important for maintaining the cell iron homeostasis, to be downregulated in the of *E. coli* Δ*tat* (Fig. 3D). Proteins YggX and Dps are known for their protective role under iron imbalance conditions in *E. coli* (Almiron et al., 1992; Pomposiello et al., 2003), so their downregulation in the cytoplasm is clearly related to the stress response. We have also observed the downregulation of several proteins important for molybdenum uptake. This unbalance in molybdenum homeostasis may be due to the dramatic decrease in DmsA, which is the largest subunit that binds molybdenum at its active site in *E. coli* (Trieber et al., 1996).

3.5. Δtat mutation provokes synthesis of colanic acid capsular polysaccharide

It has previously been observed that the Δ*tatC* strain responds to envelope stress by upregulation of genes involved in the cell envelope synthesis. Expression of the *cps* operon was shown to be induced (more than 2-fold difference compared to parental strain) only under anaerobic conditions (Ize et al., 2004). The results of our study not only showed the induction of *cps* operon proteins in Δ*tatABCDE* under aerobic conditions, but also the exclusive presence of nearly all the *cps* proteins in the *tat* mutant when compared with the parental strain. In short, we observed an induction of most of the *cps* genes responsible for the production of colanic acid, an exopolysaccharide necessary for the formation of the three-dimensional structure of *E. coli* biofilms (Danese et al., 2000). Fourteen out of 20 proteins involved in this cluster are present in our dataset, notably 13 of them only in the Δ*tat* strain (Fig. 4A–B). Of all the proteins in the *cps* cluster only one of them has a Tat signal peptide: WcaM (Stevenson et al., 1996). However, WcaM was not present in the obtained proteomic data, and neither were Wzx or WcaB/D, which were assumed to be also upregulated. These proteins are inner transmembrane proteins, which makes them highly difficult to solubilize and detect using standard proteomics. In conclusion, the identification of proteins up- and downstream from WcaM, Wzx, WcaB/D may suggest an induction of the entire *csp* operon. The fact that most of the proteins were identified only in the Δ*tat* strain, but not in the WT, strongly suggests the dependence of colanic acid formation on the Tat secretion deficiency in the cell. Moreover, the upregulation of the colanic acid synthesis in Δ*tat* was also mirrored by an increased amount of the exopolysaccharide produced by the mutant compared to WT (Fig. 4C).

3.6. Colanic acid synthesis promotes biofilm formation in E. coli Δtat

In the previous Section (3.5) we showed that the deletion of *tat* genes leads to induction of a set of proteins involved in the synthesis of colanic acid, which are not present in the wild type. Based on this observation and the fact that this exopolysaccharide is required for development of biofilm in *E. coli*, we decided to investigate biofilm formation of the *tat* mutant in comparison to wild type cells. A biofilm forms when bacteria adhere to surfaces in aqueous environments. Ultimately, a biofilm is formed to protect bacteria from stressful environmental factors, although it is known that certain cellular changes such as DNA damage, oxidative stress (Geier et al., 2008) and iron depletion (García et al., 2015) also promote biofilm development. In fact, it is often believed that any stress may trigger biofilm formation as a means of protection. To comparatively quantify biofilm formation of mutant and WT, a biofilm assay based on the ability of bacteria to adhere to plastic surface of microtiter plates was performed. To this end, cells were grown in standard LB medium to mirror the conditions of the proteomic experiment. Biofilm formation was also assessed for cells grown in minimal medium, since it has been reported that a strong biofilm formation in *E. coli* can be observed mostly in minimal media (Naves et al., 2008). Biofilm formation was defined as the intensity of crystal violet stained cells divided by optical density of the upper culture. The obtained results showed enhanced biofilm formation ability of *E. coli* Δ*tat*, especially after 48 h in both media (Fig. 5). These results may seem surprising, especially taking into account the previously reported decrease in biofilm formation of a Δ*tatC* mutant (Ize et al., 2004). Nevertheless, it has to be noted that biofilm formation is a highly complex phenomenon that is initiated via numerous pathways depending on the strain, medium and environment. Apart from the colanic acid, the presence of IBs in the *tat* mutant may account for the observed biofilm production. It has been shown that IBs formation is associated with an abnormal phenotype involving cell clustering and the development of biofilm-like characteristics (Lee et al., 2008). In conclusion, we assume that the higher biofilm-forming capacity of *E. coli* Δ*tat* is acquired as a response to stress generated by the loss of Tat-secretion and can be attributed to the upregulation of colanic acid cluster proteins in the mutant, not observed in the wild type.

4. Conclusions

We have presented a global view of cellular consequences of a *tatABCDE* deletion, that to the best of our knowledge, is so far the most comprehensive analysis of the proteome changes due to the Tat apparatus deficiency in *E. coli*. Apart from the already known filamentous chain-like phenotype of *E. coli* Δ*tat*, we identified the production of OMVs and increased inclusion body formation as novel phenotypes of *tat* mutants. Our proteomic analysis has revealed the upregulation of proteins involved in protein folding, degradation and response to heat, oxidation, osmolarity, and cold. In addition, the impairment of *E. coli* outer membrane resulted in the induction of proteins responsible for cell wall biogenesis. The *tat* deletion negatively affects the synthesis of iron and molybdenum transporters and imbalances their homeostasis in the cell. Finally, we have shown that a simultaneous deletion of *tatABCDE* genes leads to the activation of proteins responsible for colanic acid synthesis, which contributes to the biofilm formation in *tat* mutant.

Funding

This project has received funding from the European Union's Horizon 2020 research and innovation programme under the Marie

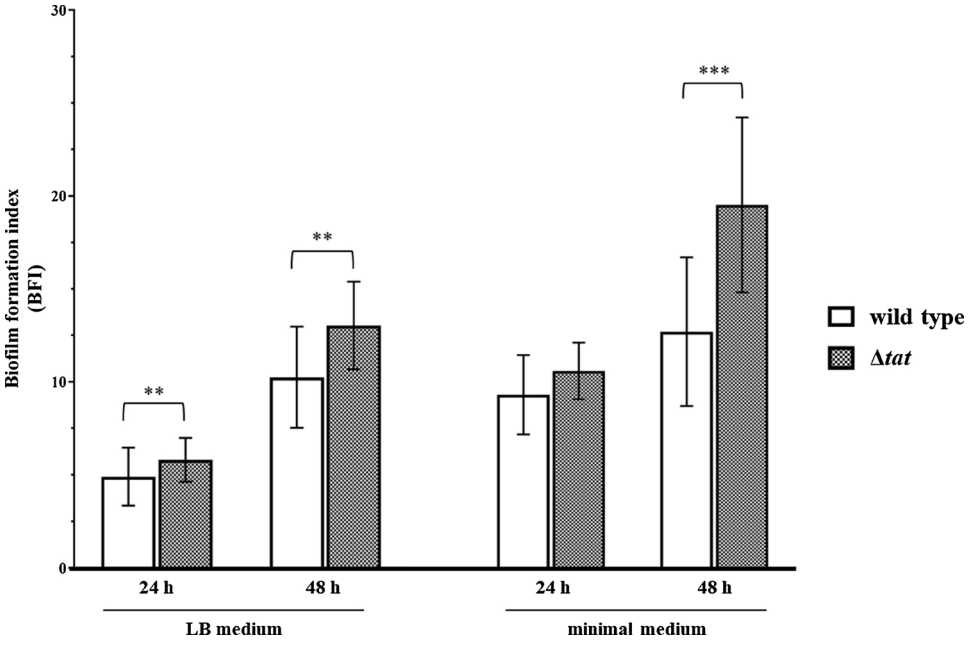

Fig. 5. Biofilm formation of *E. coli* WT and Δ*tat*. The ability to form a biofilm was assessed using a polystyrene microtiter plate biofilm assay described under "Materials and methods". Cultures were grown anaerobically in two media: LB and Belitsky minimal medium. The biofilm absorbance was measured after 24 and 48 h. Error bars indicate standard deviations calculated from 20 replicates.

Skłodowska-Curie grant agreement No. 642836.

Authors contributions

K.D. and I.G. designed and performed the experiments, analyzed the data and wrote the manuscript. W.M and C.R. devised the project. R.S. prepared specimens for microscopy and provided micrographs. T.S. and C.W. performed mass spectrometric measurements. C.R, K.R. and S.S were involved in planning and supervision of the work. All authors provided critical feedback and helped shape the research, analysis and manuscript.

Appendix A. Supplementary data

Supplementary material related to this article can be found, in the online version, at doi:https://doi.org/10.1016/j.micres.2018.10.008.

References

Ajouz, B., Berrier, C., Garrigues, A., Besnard, M., Ghazi, A., 1998. Release of thioredoxin via the mechanosensitive channel MscL during osmotic downshock of *Escherichia coli* cells. J. Biol. Chem. 273 (41), 26670–26674.

Alami, M., Trescher, D., Wu, L.F., Müller, M., 2002. Separate analysis of twin-arginine translocation (Tat)-specific membrane binding and translocation in Escherichia coli. J. Biol. Chem. 277 (23), 20499–20503.

Alami, M., Luke, I., Deitermann, S., Eisner, G., Koch, H.G., Brunner, J., Müller, M., 2003. Differential interactions between a twin-arginine signal peptide and its translocase in Escherichia coli. Mol. Cell 12, 937–946.

Aldea, M., Hernandez-Chico, H., De la Campa, A.G., Kusnher, S.R., Vicente, M., 1988. Identifcation, cloning, and expression of bolA, an ftsZ-dependent morphogene of *E. coli*. J. Bacteriol. 170, 5169–5176.

Almiron, M., Link, A.J., Furlong, D., Kolter, R., 1992. A novel DNA-binding protein with regulatory and protective roles in starved Escherichia coli. Genes Dev. 6, 2646–2654.

Baglieri, J., Beck, D., Vasisht, N., Smith, C.J., Robinson, C., 2018. Structure of TatA paralog, TatE, suggests a structurally homogeneous form of Tat protein translocase that transports folded proteins of differing diameter. J. Biol. Chem. 287, 7335–7344.

Ball, G., Antelmann, H., Imbert, P.R.C., Gimenez, M.R., Voulhoux, R., Ize, B., 2016. Contribution of the twin arginine translocation system to the exoproteome of *Pseudomonas aeruginosa*. Sci. Rep. 6, 27675.

Behrendt, J., Standar, K., Lindenstrauß, U., Bruser, T., 2004. Topological studies on the twin-arginine translocase component TatC. FEMS Microbiol. Lett. 15, 303–308.

Bendtsen, J.D., Nielsen, H., Widdick, D., Palmer, T., Brunak, S., 2005. Prediction of twin-arginine signal peptides. BMC Bioinf. 6, 167.

Berks, B.C., Palmer, T., Sargent, F., 2005. Protein targeting by the bacterial twin-arginine translocation (Tat) pathway. Curr. Opin. Microbiol. 8, 174–181.

Berks, B.C., 2015. The twin-arginine protein translocation pathway. Annu. Rev. Biochem. 84, 843–864.

Bernhardt, T.G., de Boer, P.A., 2003. The *Escherichia coli* amidase AmiC is a periplasmic septal ring component exported via the twin-arginine transport pathway. Mol. Microbiol. 48 (5), 1171–1182.

Blaudeck, N., Sprenger, G.A., Freudl, R., Wiegert, T., 2001. Specificity of signal peptide recognition in Tat-dependent bacterial protein translocation. J. Bacteriol. 183 (2), 604–610.

Blaudeck, N., Kreutzenbeck, P., Freudl, R., Sprenger, G.A., 2003. Genetic analysis of pathway specificity during posttranslational protein translocation across the *Escherichia coli* plasma membrane. J. Bacteriol. 185 (9), 2811–2819.

Bogsch, E.G., Sargent, F., Stanley, N.R., Berks, B.C., Robinson, C., Palmer, T., 1998. An essential component of a novel bacterial protein export system with homologues in plastids and mitochondria. J. Biol. Chem. 273, 18003–18006.

Brown, R.N., Romine, M.F., Schepmoes, A.A., Smith, R.D., Lipton, M.S., 2010. Mapping the subcellular proteome of *Shewanella oneidensis* MR-1 using sarkosyl-based fractionation and LC-MS/MS protein identification. J. Proteome Res. 9, 4454–4463.

Browning, D.F., Richards, K.L., Peswani, A.R., Roobol, J., Busby, S.J.W., Robinson, C., 2017. *Escherichia coli* 'TatExpress' strains super-secrete human growth hormone into the bacterial periplasm by the Tat pathway. Biotech. Bioeng. 114, 2828–2836.

Bukau, B., Walker, G.C., 1989. Cellular defects caused by deletion of the *Escherichia coli dnaK* gene indicate roles for heat shock protein in normal metabolism. J. Bacteriol. 171, 2337–2346.

Carrio, M.M., Villaverde, A., 2002. Construction and deconstruction of bacterial inclusion bodies. J. Biotechnol. 96, 3–12.

Carrió, M.M., Villaverde, A., 2005. Localization of chaperones DnaK and GroEL in bacterial inclusion bodies. J. Bacteriol. 187 (10), 3599–3601.

Collinson, I., Corey, R.E., Allen, W.J., 2015. Channel crossing: how are proteins shipped across the bacterial plasma membrane? Philos. Trans. R. Soc. Lond. B Biol. Sci. 370, 1679.

Constantinidou, C., Hobman, J.L., Griffiths, L., Patel, M.D., Penn, C.W., Cole, J.A., Overton, T.W., 2005. A reassessment of the FNR regulon and transcriptomic analysis of the effects of nitrate, nitrite, NarXL, and NarQP as *Escherichia coli* K12 adapts from aerobic to anaerobic growth. J. Biol. Chem. 281 (8), 4802–4815.

Conti, J., Viola, M.G., Camberg, J.L., 2015. The bacterial cell division regulators MinD and MinC form polymers in the presence of nucleotide. FEBS Lett. 589 (2), 201–206.

Cox, J., Mann, M., 2006. MaxQuant enables high peptide identification rates, individualized ppb-range mass accuracies and proteome-wide protein 98 quantification. Nat. Biotechnol. 26 (12), 1367–1372.

Cox, J., Neuhauser, N., Michalski, A., Scheltema, R.A., Olsen, J.V., Mann, M., 2011. Andromeda: a peptide search engine integrated into the MaxQuant environment. J. Proteome Res. 10 (4), 1794–1805.

Danese, P.N., Pratt, L.A., Kolter, R., 2000. Exopolysaccharide production is required for development of *Escherichia coli* K-12 biofilm architecture. J. Bacteriol. 182 (12), 3593–3596.

Davies, B.W., Kohanski, M.A., Simmons, L.A., Winkler, J.A., Collins, J.J., Walker, G.C., 2009. Hydroxyurea induces hydroxyl radical-mediated cell death in *Escherichia coli*. Mol. Cell 36 (5), 845–860.

DeLisa, M.P., Lee, P., Palmer, T., Georgiou, G., 2004. Phage shock protein PspA of *Escherichia coli* relieves saturation of protein export via the Tat pathway. J. Bacteriol. 186, 366–373.

Dilks, K., Rose, R.W., Hartmann, E., Pohlschröder, M., 2003. Prokaryotic utilization of the twin-arginine translocation pathway: a genomic survey. J. Bacteriol. 185 (4), 1478–1483.

Economou, A., 2005. Sec, drugs and rock'n'roll: antibiotic targeting of bacterial protein translocation. Emerg. Ther. Targets 5 (2), 141–153.

Eraso, J.M., Markillie, L.M., Mitchell, H.D., Taylor, R.C., Orr, G., Margolin, W., 2014. The highly conserved MraZ protein is a transcriptional regulator in *Escherichia coli*. J. Bacteriol. 196, 2053–2066.

Fayet, O., Ziegelhoffer, T., Georgopoulos, C., 1998. The groES and groEL heat shock gene products of *Escherichia coli* are essential for bacterial growth at all temperatures. J.

Bacteriol. 171 (3), 1379–1385.
Fröbel, J., Rose, P., Müller, M., 2012. Twin-arginine-dependent translocation of folded proteins. Philos. Trans. R. Soc. Lond. B Biol. Sci. 367, 1029–1046.
García, C.A., Alcaraz, E.S., Franco, M.A., Passerini de Rossi, B.N., 2015. Iron is a signal for *Stenotrophomonas maltophilia* biofilm formation, oxidative stress response, OMPs expression, and virulence. Front. Microbiol. 6, 926.
Geier, H., Mostowy, S., Cangelosi, G.A., Behr, M.A., Ford, T.E., 2008. Autoinducer-2 Triggers the Oxidative Stress Response in *Mycobacterium avium*, leading to biofilm formation. Appl. Environ. Microbiol. 74 (6), 1798–1804.
Gerdes, S.Y., Scholle, M.D., Campbell, J.W., Balázsi, G., Ravasz, E., Daugherty, M.D., Osterman, A.L., 2003. Experimental determination and system level analysis of essential genes in *Escherichia coli* MG1655. J. Bacteriol. 185 (19), 5673–5684.
Gottesman, S., Stout, V., 1991. Regulation of capsular polysaccharide synthesis in *Escherichia coli* K12. Mol. Microbiol. 5 (7), 1599–1606.
Hatzixanthis, K., Palmer, T., Sargent, F., 2003. A subset of bacterial inner membrane proteins integrated by the twin-arginine translocase. Mol. Microbiol. 49, 1377–1390.
Hoffmann, J.H., Linke, K., Graf, J.H., Lilie, H., Jakob, U., 2004. Identification of a redox-regulated chaperone network. EMBO J. 23 (1), 160–168.
Hussain, H., Grove, J., Griffiths, L., Busby, S., Cole, J., 1994. A seven-gene operon essential for formate-dependent nitrite reduction to ammonia by enteric bacteria. Mol. Microbiol. 12, 153–163.
Ize, B., Gerard, F., Zhang, M., Chanal, A., Voulhoux, R., Palmer, T., Filloux, A., Wu, L.F., 2002. In vivo dissection of the Tat translocation pathway in *Escherichia coli*. J. Mol. Biol. 317, 327–335.
Ize, B., Stanley, N.R., Buchanan, G., Palmer, T., 2003. Role of the *Escherichia coli* Tat pathway in outer membrane integrity. Mol. Microbiol. 48, 1183–1193.
Ize, B., Porcelli, I., Lucchini, S., Hinton, J.C., Berks, B.C., Palmer, T., 2004. Novel phenotypes of *Escherichia coli* tat mutants revealed by global gene expression and phenotypic analysis. J. Biol. Chem. 279 (46), 47543–47554.
Joliff, G., Beguin, P., Juy, M., Millet, J., Ryter, A., Poljak, R., Anbert, J.P., 1986. Isolation, crystallization and properties of a new cellulase of *Clostridium thermocellum* overproduced in *Escherichia coli*. Bio. Technol. 4, 896–900.
Jones, S.E., Lloyd, L.J., Tan, K.K., Buck, M., 2003. Secretion defects that activate the phage shock response of *Escherichia coli*. J. Bacteriol. 185, 6707–6711.
Koch, S., Fritsch, M.J., Buchanan, G., Palmer, T., 2012. *Escherichia coli* TatA and TatB Proteins Have N-out, C-in Topology in Intact Cells. J. Biol. Chem. 287 (18), 14420–14431.
Krehenbrink, M., Edwards, A., Downie, J.A., 2011. The superoxide dismutase SodA is targeted to the periplasm in a SecA-dependent manner by a novel mechanism. Mol. Microbiol. 82 (1), 164–179.
Leake, M.C., Greene, N.P., Godun, R.M., Granjon, T., Buchanan, T., Chen, S., Berry, R.M., Palmer, T., Berks, B.C., 2008. Variable stoichiometry of the TatA component of the twin-arginine protein transport system observed by in vivo single- molecule imaging. PNAS 105 (40), 15376–15381.
Lee, K.K., Jang, C.S., Yoon, J.Y., Kim, S.Y., Kim, T.H., Ryu, K.H., Kim, W., 2008. Abnormal cell division caused by inclusion bodies in *E. coli*; increased resistance against external stress. Microbiol. Res. 163 (4), 394–402.
Lee, P.A., Buchanan, G., Stanley, N.R., Berks, B.C., Palmer, T., 2002. Truncation analysis of TatA and TatB defines the minimal functional units required for protein translocation. J. Bacteriol. 184, 5871–5879.
Lee, P.A., Tullman-Ercek, D., Georgiou, G., 2006. The bacterial twin-arginine translocation pathway. Annu. Rev. Microbiol. 60, 373–395.
Méjean, V., Lobbi-Nivol, C., Lepelletier, M., Giordano, G., Chippaux, M., Pascal, M., 1994. TMAO anaerobic respiration in *Escherichia coli*: involvement of the tor operon. Mol. Microbiol. 11, 1169–1179.
Müller, M., Klösgen, R.B., 2005. The Tat pathway in bacteria and chloroplasts (review). Mol. Membr. Biol. 22, 113–121.
Muntel, J., Hecker, M., Becher, D., 2012. An exclusion list based label-free proteome quantification approach using an LTQ Orbitrap. Rapid Commun. Mass Spectrom. 26, 701–709.
Naves, P., del Prado, G., Huelves, L., Gracia, M., Ruiz, V., Blanco, J., Rodríguez-Cerrato, V., Ponte, M.C., Soriano, F., 2008. Measurement of biofilm formation by clinical isolates of *Escherichia coli* is method-dependent. J. Appl. Microbiol. 105 (2), 585–590.
Neumann, M., Mittelstädt, G., Iobbi-Nivol, C., Saggu, M., Lendzian, F., Hildebrandt, P., Leimkühler, S., 2009. A periplasmic aldehyde oxidoreductase represents the first molybdopterin cytosine dinucleotide cofactor containing molybdo-flavoenzyme from Escherichia coli. FEBS J. 276 (10), 2762–2774.
Obadia, B., Lacour, S., Doublet, P., Baubichon-Cortay, H., Cozzone, A.J., Grangeasse, C., 2007. Influence of tyrosine-kinase Wzc activity on colanic acid production in *Escherichia coli* K12 cells. J. Mol. Biol. 367, 42–53.
Ochsner, U.A., Snyder, A., Vasil, A.I., Vasil, M.L., 2002. Effects of the Twin-arginine translocase on secretion of virulence factors, stress response, and pathogenesis. Proc. Natl. Am. Sci. U. S. A. 99 (12), 8312–8317.
Orfanoudaki, G., Economou, A., 2014. Proteome-wide subcellular topologies of *E. coli* polypeptides database (STEPdb). Mol. Cell Proteomics 13 (12), 3674–3687.
O'Toole, G.A., 2011. Microtiter dish biofilm formation assay. J. Vis. Exp. 47, 2437.
Overbeek, R., Olson, R., Pusch, G.D., Olsen, G.J., Davis, J.J., Disz, T., Edwards, R.A., Gerdes, S., Parrello, B., Shukla, M., Vonstein, V., Wattam, A.R., Xia, F., Stevens, R., 2014. The SEED and the rapid annotation of microbial genomes using subsystems technology (RAST). Nucleic Acids Res. 42, 206–214.
Palmer, T., Sargent, F., Berks, B.C., 2005. Export of complex cofactor-containing proteins by the bacterial Tat pathway. Trends Microbiol. 13 (4), 175–180.
Patel, R., Smith, S.M., Robinson, C., 2014. Protein transport by the bacterial Tat pathway. Biochim. Biosphys. Acta – Mol. Cell. Res. 1843, 1620–1626.
Petriman, N.A., Jauß, B., Hufnagel, A., Franz, L., Sachelaru, I., Drepper, F., Warscheid, B., Koch, H.G., 2018. The interaction network of the YidC insertase with the SecYEG translocon, SRP and the SRP receptor FtsY. Sci. Rep. 8 (578).
Pierce, J.J., Turner, C., Keshavarz-Moore, E., Dunnill, P., 1997. Factors determining more efficient large-scale release of a periplasmic enzyme from *E. coli* using lysozyme. J. Biotechnol. 58 (1), 1–11.
Pomposiello, P.J., Koutsolioutsou, A., Carrasco, D., Demple, B., 2003. SoxRS-regulated expression and genetic analysis of the yggX gene of *Escherichia coli*. J. Bacteriol. 185, 6624–6632.
Pradel, N., Ye, C., Livrelli, V., Xu, J., Joly, B., Wu, L., 2003. Contribution of the twin arginine translocation system to the virulence of enterohemorrhagic *Escherichia coli* O157:H7. Infect. Immun. 71, 4908–4916.
Rabilloud, T., 2012. Limits of Proteomics: Protein Solubilisation Issues. eLS. .
Randall, L.L., Hardy, J.S., 1986. Correlation of competence for export with lack of tertiary structure of the mature species: a study in vivo of maltose-binding protein in *E. coli*. Cell 12, 921–928.
Rappsilber, J., Mann, J., Ishihama, Y., 2007. Protocol for micro-purification, enrichment, pre-fractionation and storage of peptides for proteomics using StageTips. Nat. Protoc. 2, 1896–1906.
Robinson, C., Bolhuis, A., 2001. Protein targeting by the twin-arginine translocation pathway. Nat. Rev. Mol. Cell Biol. 2, 350–356.
Rodrigue, A., Chanal, A., Beck, K., Muller, M., Wu, L.F., 1999. Co-translocation of a periplasmic enzyme complex by a hitchhiker mechanism through the bacterial Tat pathway. J. Biol. Chem. 274 (19), 13223–13228.
Rose, P., Förbel, J., Graumann, P.L., Müller, M., 2013. Substrate-dependent assembly of the tat translocase as observed in live *escherichia coli* cells. PLoS One 8 (8), e69488.
Sawers, R.G., Boxer, D.H., 1986. Purification and properties of membrane-bound hydrogenase isoenzyme 1 from anaerobically grown *Escherichia coli* K12. Eur. J. Biochem. 156, 265–275.
Schröder, H., Langer, T., Hartl, F.U., Bukau, B., 1993. DnaK, DnaJ and GrpE form a cellular chaperone machinery capable of repairing heat-induced protein damage. EMBO J. 12 (11), 4137–4144.
Stanley, N.R., Palmer, T., Berks, B.C., 2000. The Twin arginine consensus motif of Tat signal peptides is involved in Sec- independent protein targeting in *Escherichia coli*. J. Biol. Chem. 275, 11591–11596.
Stanley, N.R., Findlay, K., Berks, B.C., Palmer, T., 2001. *Escherichia coli* strains blocked in tat-dependent protein export exhibit pleiotropic defects in the cell envelope. J. Bacteriol. 183, 139–144.
Stanley, N.R., Sargent, F., Buchanan, G., Shi, J., Stewart, V., Palmer, T., Berks, B.C., 2002. Behaviour of topological marker proteins targeted to the Tat protein transport pathway. Mol. Microbiol. 43, 1005–1021.
Stevenson, G., Andrianopoulos, K., Hobbs, M., Reeves, P.R., 1996. Organization of the *Escherichia coli* K-12 gene cluster responsible for production of the extracellular polysaccharide colanic acid. J. Bacteriol. 178 (16), 4885–4893.
Stülke, J., Hanschke, R., Hecker, M., 1993. Temporal activation of beta-glucanase synthesis in *Bacillus subtilis* is mediated by the GTP pool. J. Gen. Microbiol. 139, 2041–2045.
Summer, E.J., Mori, H., Settles, A.M., Cline, K., 2000. The thylakoid ΔpH-dependent pathway machinery facilitates RR-independent N-tail protein integration. J. Biol. Chem. 275, 23483–23490.
Sutherland, G.A., Grayson, K.J., Adams, N.B.P., Mermans, D.M.J., Jones, A.S., Robertson, A.J., Auman, D.B., Brindley, A.A., Sterpone, F., Tufferye, P., Derreumaux, P., Dutton, P.L., Robinson, C., Hitchcock, A., Hunter, C.N., 2018. Probing the quality control mechanism of the *Escherichia coli* twin-arginine translocase with folding variants of a de novo-designed heme protein. J. Biol. Chem. 293, 6672–6681.
Takahashi, Y., Nakamura, M., 1999. Functional assignment of the ORF2-iscS-iscU-iscA-hscB-hscA-fdx-ORF3 gene cluster involved in the assembly of Fe-S clusters in *Escherichia coli*. J. Biochem. 126 (5), 917–926.
Thomas, J.G., Baneyx, F., 2000. ClpB and HtpG facilitate de novo protein folding in stressed *Escherichia coli* cells. Mol. Microbiol. 36 (6), 1360–1370.
Tinker, J.K., Erbe, J.L., Holmes, R.K., 2005. Characterization of fluorescent chimeras of cholera toxin and *Escherichia coli* heat-labile enterotoxins produced by use of the twin arginine translocation system. Infect. Immun. 73 (6), 3627–3635.
Trieber, C.A., Rothery, R.A., Weiner, J.H., 1996. Consequences of removal of a molybdenum ligand (DmsA-Ser-176) of *Escherichia coli* dimethyl sulfoxide reductase. J. Biol. Chem. 271 (44), 27339–27345.
Tullman-Ercek, D., DeLisa, D., Kawarasaki, Y., Iranpour, P., Ribnicky, B., Palmer, T., Georgiou, G., 2007. Export pathway selectivity of *Escherichia coli* twin arginine translocation signal peptides. J. Biol. Chem. 282, 8309–8316.
Walker, K.L., Jones, A.S., Robinson, C., 2015. The Tat pathway as a biotechnological tool for the expression and export of heterologous proteins in *Escherichia coli*. Pharm. Bioprocess. 3 (6), 387–396.
Wexler, M., Sargent, F., Jack, R.L., Stanley, N.R., Bogsch, E.G., Robinson, C., Berks, B.C., Palmer, T., 2000. TatD is a cytoplasmic protein with DNase activity. No requirement for TatD family proteins in sec-independent protein export. J. Biol. Chem. 275 (22), 16717–16722.
Wolff, S., Hahne, H., Hecker, M., Becher, D., 2008. Complementary analysis of the vegetative membrane proteome of the human pathogen Staphylococcus aureus. Mol. Cell Proteomics 7 (8), 1460–1468.
Yaagoubi, A., Kohiyama, M., Richarme, G., 1994. Localization of DnaK (chaperone 70) from *Escherichia coli* in an osmotic-shock-sensitive compartment of the cytoplasm. J. Bacteriol. 176 (22), 7074–7078.
Zühlke, D., Dörries, K., Bernhardt, J., Maaß, S., Muntel, J., Liebscher, V., Pané-Farré, J., Riedel, K., Lalk, M., Völker, U., Engelmann, S., Becher, D., Fuchs, S., Hecker, M., 2016. Costs of life–dynamics of the protein inventory of *Staphylococcus aureus* during anaerobiosis. Sci. Rep. 6, 28172.